EARTH OBSERVATION AND GEOMATICS ENGINEERING
website: https://eoge.ut.ac.ir

# A Method for Improvement of PDR method using Smartphones Considering Pedestrian Properties

**Boshra Khalili[1], Rahim Ali Abbaspour[2], Alireza Chehreghan[3]***

[1,2] School of Surveying and Geo-spatial Engineering, College of Engineering, University of Tehran, Tehran, Iran
[3]Mining Engineering Faculty, Sahand University of Technology, Tabriz, Iran

**Article history:**

Received: 2023-03-17, Accepted: 2023-05-01, Published: 2023-06-14

## ABSTRACT

Indoor positioning is one of the most challenging issues in location-based services. Smartphone-based Pedestrian Dead Reckoning (PDR) is commonly used as an indoor positioning system because it does not require infrastructure. The positioning estimation errors, however, are cumulatively increased over time. In this approach, step length estimation error is one of the main sources of positioning error. In this study, to improve indoor positioning accuracy using smartphone-embedded sensors, the pedestrian's gender and walking speed are considered effective factors in adjusting the parameters of step length estimation methods. Accordingly, collected data are divided into six classes based on walking speed (high, medium, low) and gender (female, male). K-Nearest Neighbors (KNN), Support Vector Machine (SVM), and Decision Trees (DTree) algorithms are adopted for classification. The classification accuracy of each of the KNN, SVM, and DTree algorithms are 93.4%, 92.4%, and 76.6% respectively. Moreover, the peak detection method is applied to identify the pedestrian's steps, and Weinberg and Ladetto methods are adopted to estimate step length. Step detection accuracy was 99.015%. Also, the error of step length estimations using Weinberg and Ladetto methods are 2.48% and 1.95%, respectively. In addition, the Extended Kalman Filter (EKF) filter is used for heading estimation, and fast walking results in the highest heading estimation error for both males and females. The mean and STD of the heading estimation error using EKF algorithms are 2.97 degrees and 2.99 degrees, respectively. In the final, the pedestrian's position is estimated according to the PDR method using estimated step lengths and estimated headings. Along a 25.8-meter path, using the Weinberg method for step length estimation, the average absolute and relative positioning errors are 0.76 and 2.95%, respectively. Moreover, using Ladetto s method for step length estimation, the average absolute and relative positioning errors are 0.92 and 3.57%, respectively.

**Keywords**

Indoor Positioning
PDR
Step Length Estimation
Classification
Machine Learning

## 1. Introduction

For outdoor positioning, GPS can be adopted (Li et al., 2012; Zhuang et al., 2015). However, GPS signals are blocked, weakened, or reflected inside the building (Groves, 2015; Huang et al., 2020; Pratama & Hidayat, 2013). Therefore, other approaches including ultra-wideband (UWB) (Otim et al., 2020; Zhou et al., 2021), Bluetooth (Bencak et al., 2022; Daníş et al., 2021) , and WLAN-based (Yang & Shao, 2015) are adopted for indoor positioning. While mentioned techniques require additional infrastructure, positioning based on Pedestrian Dead Reckoning (PDR) is infrastructure-free (Li et al., 2012; Nilsson et al., 2013). Step detection, estimating step length, and determining heading are the fundamental components of PDR positioning. In the smartphone-based PDR method, data are collected from various smartphone-embedded sensors including the accelerometer, gyroscope, and magnetometer, and the current position is estimated based on estimated step lengths, estimated headings, and position of the previous step. Step length estimation errors and

* Corresponding author
E-mail addresses: chehreghan@sut.ac.ir

heading estimation errors are the two main sources of positioning error in the PDR method (Munoz Diaz et al., 2017). Accordingly, since positioning error increase cumulatively, positioning accuracy is significantly affected by errors with PDR method (Jin et al., 2011; Woodman, 2007; Wu et al., 2018).

A crucial factor in PDR positioning is heading estimation, as it contributes significantly to positioning's cumulative error. As gyroscope sensors' data contains a high level of noise, they can cause significant errors if used for long-term heading estimation Therefore, accelerometer and magnetometer sensors are also employed to decrease heading estimation errors (Metge et al., 2014). In addition, Magnetic disturbance can cause considerable errors in heading estimation (Li et al., 2021). Accordingly, Various methods have been proposed to reduce heading estimation errors. Zhao et al. (2019) reduced heading estimation errors to less than 4 degrees using the GDA algorithm. Li et al. (Li et al., 2021) applied the Kalman filter to decline magnetic disturbances. Furthermore, they mitigated the cumulative error in positioning resulting from heading estimation by employing the Zero Lateral Displacement Update optimization technique. In this method, the heading estimation and positioning errors were 2 degrees and 2 m, respectively.

Furthermore, the identification of steps plays a crucial role in Pedestrian Dead Reckoning (PDR) positioning. Numerous techniques utilizing acceleration have been suggested, including the thresholds setting, peak identification, and correlation analysis. (Jang et al., 2007; Sheu et al., 2014). Moreover, step length estimation plays a pivotal role in PDR positioning. There are various methods for step length estimation including acceleration's integral methods, deep learning-based methods, and computational models (Luo et al., 2020). The main advantage of acceleration's integral methods is that they do not require a training process or training data which are collected from individuals with distinctive characteristics. However, since the smartphone-embedded sensors are not accurate enough, acceleration's integral methods do not estimate step lengths accurately (Díez et al., 2018). In addition, deep-learning-based step length estimation methods are applied using deep-learning algorithms and various sensor data. The major advantage of this method is that it requires one to be trained only once. However, requiring a large number of training data and complicated implementation are its main drawbacks (Gu et al., 2018).

Many studies have utilized computational models for step-length estimation. Ladetto (2000) proposed a method using acceleration's frequency and variance to estimate step length. In addition, Weinberg (2002) used the steps' maximum and minimum acceleration values of the Z-axis for step length estimation. Kim et al. (2004) employed an approach by utilizing the average acceleration value of steps to accurately estimate the length of each individual step. Since the methods are not computationally complex, they are easy to implement on smartphones. However, these methods have several parameters that should be adjusted based on different individuals' characteristics and movement habits (Díez et al., 2018). Lu et al. (2020) developed a fuzzy controller utilizing the fuzzy logic algorithm to estimate the coefficient of Weinberg's constant, considering various walking speeds. The average step length error of five pedestrians was less than 4 m of the 100 m path. Moreover, Huang et al. (2022) estimated step length based on nonlinear regression models of extracted features of five phases of the step. The relative error of the step length estimation of various walking speeds was less than 2%. To improve positioning accuracy, Klein et al. (2018) used machine learning algorithms to classify phone-carrying modes and adjust the step length estimation models accordingly. Wu et al. (2021) also identified six pedestrian activities using machine learning algorithms and adjusted Weinberg's constant coefficient accordingly. The average positioning error was 1.79 meters in a multi-story building. A movement's speed affects the domain of acceleration data, and acceleration data in turn affects the step length. Furthermore, since the step length of females and males differs, gender should be considered in adjusting step length parameters. Khalili et al. (2022) proposed an adaptive Pedestrian Dead Reckoning (PDR) approach to tackle challenges related to smartphone-carrying modes, pedestrian activities, and movement speeds. They utilized SVM and DTree algorithms for motion state and walking speed identification. However, they did not incorporate matching learning algorithms for gender recognition and only the Weinberg method was used for step length estimation. whereas, this study applies a classification technique based on machine learning to effectively distinguish between males and females at varying walking speeds. Utilizing matching learning algorithms for motion recognition, specifically in gender recognition for Pedestrian Dead Reckoning (PDR), brings significant advantages including increased accuracy, enhanced classification of gender-based motion patterns, and superior performance compared to methods that do not employ matching learning techniques. In addition, step length was estimated using Weinberg and Ladetto methods. To increase the accuracy of positioning, the step length parameters are adjusted based on gender and movement speed, since these factors have a significant influence on adjusting step length parameters. This paper is organized as follows: Section 2 outlines the proposed method and associated details. The third section of the paper provides a comprehensive overview of the proposed PDR positioning algorithm. In the fourth section, the results are presented, and suggestions for future research directions are provided.

## 2-Proposed method

As shown in Figure (1), This study proposes the PDR method, which involves multiple stages. Initially, raw data were collected with accelerometer, gyroscope, and magnetometer smartphone-embedded sensors. Furthermore, to enhance the quality of the signals used in the system, a low-pass filter was implemented to eliminate high-frequency noise from both the acceleration and gyroscope signals. Additionally, for accurate magnetometer readings, an ellipsoidal model approach was employed for magnetometer calibration. Since the pre-processing data was insufficient to distinguish one motion mode from other modes, time-domain features were extracted from acceleration and angular velocity data in each time window. In the following, the acceleration-based peak detection algorithm, both Weinberg and Ladetto algorithms, and the Extended Kalman filter (EKF) (Einicke & White, 1999) were applied to step detection, step length estimation, and heading estimation, respectively (Goyal et al., 2011). Finally, the pedestrian's position was estimated based on the pedestrian's initial position, estimated step lengths, and headings.

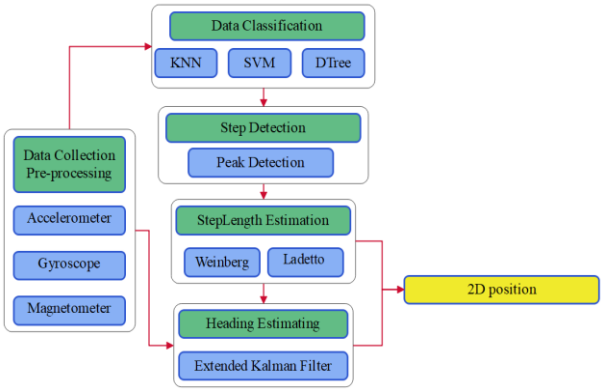


Figure 1. The proposed PDR system's structure.

According to (1) and (2), in the PDR positioning, the current pedestrian's location is determined based on the pedestrian's location, estimated step length, and estimated heading in the previous step (Deng et al., 2015).

$$\boldsymbol{X_i = X_{i-1} + L_i \times cos\,\Psi_i} \quad (1)$$

$$\boldsymbol{Y_i = Y_{i-1} + L_i \times sin\,\Psi_i} \quad (2)$$

where $X_i$ and $Y_i$ are the coordinates representing the location of the pedestrian in step I. Also, at step in, $L_i$ and $\Psi_i$ are the length and direction of the pedestrian's movement, respectively. The initial location of the pedestrian is either pre-set by default or determined by scanning QR codes in the building.

### 2-1-Data Collection and Calibration

Data were collected using smartphone-embedded sensors including an accelerometer, gyroscope, and magnetometer with a sampling rate of 100 samples per second. The measured data contained several errors such as bias error and random noise. Also, magnetic disturbances caused hard iron and soft iron errors in magnetic data. Accordingly, since the positioning error increased cumulatively over time, the accuracy of the final estimated location decreased. Therefore, it was necessary to identify and eliminate the errors in measured data. A bias error is a difference between measured and actual values, which is one of the errors of measured data. The bias error is modeled as matrix b in (3) (Jurman et al., 2007; Olivares et al., 2013).

$$\mathrm{b} = \begin{bmatrix} \mathrm{b_x} \\ \mathrm{b_y} \\ \mathrm{b_z} \end{bmatrix} \quad (3)$$

where $b_x$, $b_y$, and $b_z$ are the bias values in the x, y, and z-axis, respectively. A scale factor error also refers to the ratio of input to output data in the measured data of smartphone sensors. This error is modeled as an SF matrix in (4) (Jurman et al., 2007; Olivares et al., 2013).

$$\mathrm{SF} = \begin{bmatrix} 1+\mathrm{sf_x} & 0 & 0 \\ 0 & 1+\mathrm{sf_y} & 0 \\ 0 & 0 & 1+\mathrm{sf_z} \end{bmatrix} \quad (4)$$

where $sf_x$, $sf_y$, and $sf_z$ are the scale factor values in the x, y, and z axis, respectively. In this measurement data, there was also random noise that may be associated with sensor characteristics or external factors. To eliminate high-frequency noise, it was necessary to apply a low-pass filter on the data. The low-pass filter (cutoff frequency 5 Hz - order 6) was applied to the acceleration data. Besides the mentioned errors, undesirable magnetic fields also caused hard iron and soft iron errors. The hard iron error appears due to the permanent magnetic field and its effects are like bias. The soft iron error also appears due to materials that affect the magnetic field but does not necessarily create the magnetic field itself (Ozyagcilar, 2012). In (5), a mathematical model for modeling the magnetic error is shown (Olivares et al., 2013; Pylvänäinen, 2008).

$$\mathrm{h_m} = \mathrm{A} \times (\mathrm{h} - \mathrm{b}) \quad (5)$$

where $h$ and $h_m$ are real and measured magnetic fields, respectively. Matrices A and b are also considered for modeling soft and hard iron errors, respectively.

### 2-2-Data Classification

The collected data after preprocessing is divided into six distinct categories according to pedestrians' gender (male and female) and the pedestrians' movement speeds (slow, medium, and high). During data collecting, pedestrians are not advised in advance about which speeds to use, and the speeds are determined by their movement habits. Based on this classification, six categories including walking at low, medium, and high speeds of each gender have been considered. Since texting mode is more common than other

modes in the indoor environment, this smartphone-carrying mode was considered (Figure 2).

Figure 2. Carrying a smartphone in texting mode

As shown in Figure (3), a smartphone is equipped with a variety of sensors such as a light sensor, sound sensor, accelerometer, gyroscope, magnetometer, and barometer. To carry out this research, three distinct types of sensors including an accelerometer, gyroscope, and magnetometer were used, and data were collected with a sampling rate of 100 samples per second.

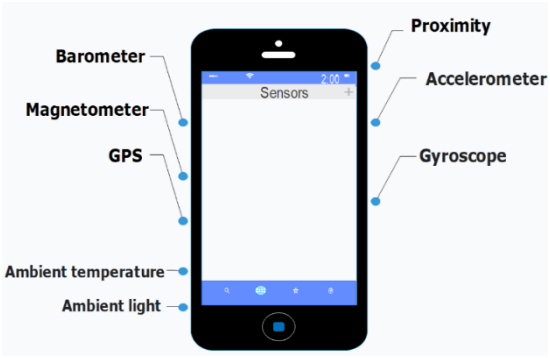


Figure 3. smartphone's sensors

**2-2-1- Features Extraction and Classification Algorithm**

For data classification, six categories were considered, including walking at low, medium, and high speeds for each gender. The pre-processed data is not adequate to differentiate between different types of motion. To this end, features including the difference of maximum and minimum, mean, variance, zero crossing rate, and skewness of the acceleration and angular velocity of three x, y, and z axis in each time window were extracted. Data were classified using the K-Nearest Neighbors (KNN) algorithm based on pedestrian movement speeds (low, medium, high) and genders (male, female). The KNN algorithm is a supervised and non-parametric machine learning technique applied for both classification and regression problems. A sample is assigned to the closest class based on similarity criteria (distance measurement) (Fang et al., 2016). In this paper, the KNN algorithm utilizes the Euclidean distance as the distance metric, and the value of K is set to 3. The accuracy of the KNN algorithm has been compared with two other classification algorithms including DTree (Elhoushi et al., 2015) and SVM (Martinelli et al., 2017). A DTree consists of nodes, specifically leaf nodes and decision nodes. Leaf nodes represent decisions and hold the classification values, while decision nodes represent attributes or class labels. The parameters of the DTree model were estimated using the recognized gender of the pedestrian and their identified walking speed. The criterion parameter was set to Gini to minimize impurity, while the maximum depth was limited to five to avoid overfitting. SVM is a machine learning algorithm utilized for both classification and regression purposes. SVM employs different kernel functions to transform input data into a higher-dimensional space, enabling the identification of an optimal hyperplane that effectively separates data into distinct classes. The paper utilizes the radial basis function kernel as the chosen kernel function for the SVM.

**2-3- Step Detection**

The peak detection method was used to recognize the pedestrian's steps (Jang et al., 2007). In Figure (4), the blue points and the blue curves are the peak points and the acceleration value, respectively. Three threshold values were used to determine the peak and valley acceleration points for step detection. The first threshold was the peak threshold, and peak points were recognized when acceleration values exceeded this threshold. The second threshold was the peak-valley threshold, and steps were valid if the difference between their peaks and valleys exceeded this threshold. Finally, steps were detected if the time interval between two consecutive steps exceeded the third threshold, which was the time threshold.

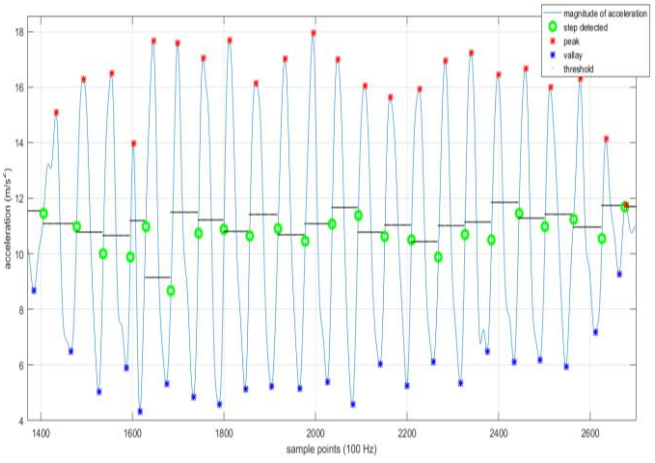


Figure 4. Step detection algorithm

**2-4- Step Length Estimation**

Different approaches can be used to calculate the stride length of pedestrians. The computational model is one of the most popular methods of estimating the pedestrian's step length in the PDR. Since the computational model is less computationally complex, it is easily implemented on a smartphone. The step length computational model's parameters can be either set to adjust automatically or manually. In this study, an automatic approach was used,

and the algorithm was trained using data collected from different pedestrians. To increase the accuracy of parameters' adjustment, individuals of various genders, heights, and ages have participated to collect training data. The parameters of these step length models were modified according to the pedestrian's movement speeds and gender. Two computational models based on acceleration were used, including Weinberg and Ladetto. In (6) and (7), Weinberg (Weinberg, 2002) and Ladetto (Ladetto, 2000) step-length models are shown, respectively.

$$S = K \times \sqrt[4]{a_{Max} - a_{Min}} \quad (6)$$

where $a_{Max}$ and $a_{Min}$ are the maximum and minimum acceleration during one step, respectively. In addition, K is Weinberg models' parameters. The least squares method was also used to adjust K based on the pedestrian's characteristics and walking speeds.

$$S = P_{10} \times F + P_{01} \times V + P_{00} \quad (7)$$

where F and V are the frequency and variance of acceleration during one step, respectively. Also, $P_{00}$ , $P_{01}$, and $P_{10}$ are models' parameters.

**2-5- Heading estimating**

The representation of an orientation or attitude in three-dimensional space can be expressed with Euler angles and quaternions. Euler angles represent an orientation or attitude in three-dimensional space using three angles, termed yaw, pitch, and roll. The values for the angles are derived from the rotation matrix through a sequence of three individual rotations. In this paper, the heading was estimated using the EKF algorithm based on the quaternion rotation. Since Euler angles may cause singularity problems and make the heading estimation process more complex, quaternion has been used to determine the device's orientation. In (8), the normalized quaternion is represented with q.

$$q = q_0 + q_1\hat{x} + q_2\hat{y} + q_3\hat{z} \quad (8)$$

where $q_0$ is the scalar part and $q_1$, $q_2$ and $q_3$ are the quaternion vector parts. Collected data, including acceleration and angular velocity, were measured in the smartphone coordinate system. In (9), the matrix that describes the transformation of the smartphone coordinate system to the global coordinate system is displayed (Diebel, 2006). Using (10), the heading can be calculated by comparing the rotational matrix derived from the Euler angles to the rotational matrix computed from the quaternion.

$$R_N^B = \begin{bmatrix} q_0^2+q_1^2-q_2^2-q_3^2 & 2(q_1q_2+q_0q_3) & 2(q_1q_3-q_0q_2) \\ 2(q_1q_2-q_0q_3) & q_0^2-q_1^2+q_2^2-q_3^2 & 2(q_0q_1+q_2q_3) \\ 2(q_1q_3+q_0q_2) & 2(q_2q_3-q_0q_1) & q_0^2-q_1^2-q_2^2+q_3^2 \end{bmatrix} \quad (9)$$

$$yaw = \tan^{-1}\left(\frac{2(q_2q_3-q_0q_1)}{q_0^2-q_1^2+q_2^2-q_3^2}\right) \quad (10)$$

The acceleration model is shown in (11) [36].

$$\widehat{q_{k+1}} = q_{k+1}^- + K_{k+1}(a_{k+1} - R_N^B(q_{k+1}^-)g + e_{k+1}^a) \quad (11)$$

where the $g$ is the gravity vector in the global coordinate system, and $a_{k+1}$and $e_{k+1}^a$ are the acceleration vector and the accelerometer's noise, respectively. Since the equation is non-linear, The EKF approach linearizes the right side of the equation (11) by calculating the Jacobian matrix. In addition, the actual value of $q_{k+1}$ is unknown in this equation, its value is replaced by its previously estimated value, $q_{k+1}^-$. Therefore, the estimation model can be linearized according to the (12) (Deng et al., 2015).

$$H_{k+1} = \frac{\partial}{\partial q_{k+1}} a_{k+1}|_{q_{k+1}=q_{k+1}^-} \quad (12)$$

Using the EKF approach, heading estimation requires calculating posterior state estimation values $\widehat{q_{k+1}}$ and its corresponding covariance matrix $P_q^{k+1}$. Therefore, at first, the previous state and the related error covariance matrix are calculated with (13) and (14) (Deng et al., 2015).

$$q_{k+1}^- = A_k\widehat{q_k} \quad (13)$$

$$P_{q^-}^{k+1} = A_k P_q^k {A_k}^T + Q_k \quad (14)$$

where $\widehat{q_k}$ and $P_q^k$ are the posterior state and its covariance matrix in the previous step, respectively. Also, $q_{k+1}^-$ and $P_{q^-}^{k+1}$ are the previous state estimation and its corresponding covariance matrix, respectively. The matrix $A_k$ and $S(w)$ are also calculated according to the (15) and (16) (Wu et al., 2018).

$$A_k = I_{4\times4} + \frac{T}{2} \times S(w) \quad (15)$$

$$S(w) = \begin{bmatrix} 0 & -w_k^x & -w_k^y & -w_k^z \\ w_k^x & 0 & w_k^z & -w_k^y \\ w_k^y & -w_k^z & 0 & w_k^x \\ w_k^z & w_k^y & -w_k^x & 0 \end{bmatrix} \quad (16)$$

where wk are the values of the angular velocity of each of the X, Y, and Z axis. Also, $I$ and $T$ are the Identity matrix and the period between samples $k$ +1 and $k$, respectively. Then the Kalman coefficient is estimated with (17) (Deng et al., 2015).

$$K_{k+1} = \frac{P_{q^-}^{k+1} {H_k}^T}{H_{k+1}P_{q^-}^{k+1}{H_{k+1}}^T + R_k} \quad (17)$$

where $R_k$ the estimated variance. Then, the posterior state $\widehat{q_{k+1}}$ and its corresponding covariance matrix $P_q^{k+1}$ are estimated with (18) and (19) (Deng et al., 2015).

$$\widehat{q_{k+1}} = q_{k+1}^- + K_{k+1}(a_{k+1} - R_N^B(q_{k+1}^-)g) \quad (18)$$

$$P_q^{k+1} = P_{q^-}^{k+1} - K_{k+1}H_{k+1}P_{q^-}^{k+1} \quad (19)$$

After estimating $\widehat{q_{k+1}}$, the pedestrian's heading can be estimated using (10).

**3- Positioning Experiment and Evaluation of Results**

Raw data were collected with smartphone-embedded sensors including an accelerometer, gyroscope, and magnetometer for positioning with the PDR method. The parameters of the step length models were adjusted based on the pedestrians' genders and movement speeds, so individuals of different genders, heights, and ages collected training data. To this end, 18 females and 14 males participated in the data collection. In Table (1), pedestrians' age is reported. Also, In Table (2), pedestrians' height is reported for both males and females. As shown in Tables (1) and (2), individuals with a wide range of ages and heights participated in data collection.

Table 1. Experimenters' age

| **Age** | **15-18** | **18-24** | **24-30** | **30-36** | **36-46** | **46-56** |
|---|---|---|---|---|---|---|
| Female | 3 | 7 | 1 | 0 | 4 | 3 |
| Male | 0 | 8 | 1 | 3 | 0 | 2 |

Table 2. Experimenters' height

| **Height (cm)** | **150-160** | **160-170** | **170-180** | **180-190** |
|---|---|---|---|---|
| Female | 3 | 13 | 2 | 0 |
| Male | 0 | 1 | 8 | 5 |

**3-1- Data Classification**

The combination of six states including two genders (female, and male) and three movement speeds (fast, normal, and slow) was considered as different states. To collect data, 18 females and 14 males walked across low, medium, and high speeds. More details about participants are reported in Tables (1) and (2). Data were split into two-second windows (samples) containing two hundred data points in each, with a 50% overlap coming from the accelerometer and gyroscope sensors. In total, 1443 samples were collected. For females, 199, 260, and 297 samples and for males, 206, 240, and 241 samples were collected at high, medium, and low speeds, respectively. To validate the classification algorithm 5fold Cross Validation method was used (Moreno-Torres et al., 2012). The accuracy of KNN, SVM, and DTree algorithms is reported in Table (3). According to Table (3), the KNN classification algorithm with an average accuracy of 93.2% and a standard deviation of 0.41%, performed better than the other two algorithms.

Table 3. Comparison accuracy of three classification algorithms

| Method | 1 | 2 | 3 | 4 | 5 | Mean | STD |
|---|---|---|---|---|---|---|---|
| KNN | 93.4% | 93.2% | 93.8% | 93.8% | 93.2% | 93.2% | 0.4% |
| SVM | 92.4% | 92.1% | 91.2% | 91.2% | 91.7% | 91/7% | 0.63% |
| DTree | 76.6% | 90.2% | 75.8% | 76.5% | 74.9% | 76.8% | 0.69% |

The confusion matrix of the KNN classification algorithm is reported in Table (4) and the number of samples reported in Table (5). In these tables, high, medium, and low walking speeds are indicated by F1, F2, and F3 for females, and M1, M2, and M3 for males. According to Table (4), the data related to categories F1 and M1 were distinguished with 100% accuracy. Nevertheless, 3.4% of instances of the F2 were misrecognized as the F3. In addition, 2.1% of instances of the M1 were misrecognized as the F3. Moreover, 6.3% of instances of the M2 were wrongly identified as other categories.

Table 4. Confusion Matrix of KNN classification

| | **F1** | **F2** | **F3** | **M1** | **M2** | **M3** |
|---|---|---|---|---|---|---|
| F1 | 100% | 0% | 0% | 0% | 0% | 0% |
| F2 | 0% | 96.6% | 3.4% | 0% | 0% | 0% |
| F3 | 0% | 3.4% | 96.6% | 0% | 0% | 0% |
| M1 | 0% | 0% | 0% | 100% | 0% | 0% |
| M2 | 0% | 0% | 2.1% | 2.1% | 93.8% | 2.1% |
| M3 | 0% | 0% | 2.1% | 0% | 0% | 97.9% |

Table 5. Number of samples according confusion matrix

| | **F1** | **F2** | **F3** | **M1** | **M2** | **M3** |
|---|---|---|---|---|---|---|
| F1 | 199 | 0 | 0 | 0 | 0 | 0 |
| F2 | 0 | 250 | 9 | 0 | 0 | 0 |
| F3 | 0 | 0 | 287 | 10 | 0 | 0 |
| M1 | 0 | 0 | 0 | 206 | 0 | 0 |
| M2 | 0 | 0 | 5 | 5 | 225 | 5 |
| M3 | 0 | 0 | 5 | 0 | 0 | 236 |

**3-2- The Implementation of PDR Positioning Algorithms**

Different parts of the PDR method including step detection, step length estimation, and heading estimation were implemented considering various walking speeds and genders to improve the robustness of PDR positioning using smartphone-embedded sensors.

**3-2-1- Step Detection**

To assess the accuracy of the step detection algorithm, three females and three males of different heights, weights and ages walked along a 35 m rectangular path at slow, normal, and fast speeds. The mean height and age of the women were respectively 167.1 ± 4.5 cm and 24.5 ± 3.1 years, while those of the men were respectively 32.2 ± 4.3 years and 181.6 ± 7.7 cm. To implement the step detection algorithm, the acceleration data collected was processed with a low-pass filter (cutoff frequency equal to 5 Hz) and the peak detection algorithm was applied. In this method, the value of three thresholds including peak threshold, peak-valley threshold, and time threshold were 11 m/$s^2$, 1.5 m/$s^2$, and 0.2 s, respectively. In Table (6), the step detection accuracies of males and females are reported and the step detection error is less than 2% in all six classes, and the average accuracy is 99.015%.

Table 6. Step detection accuracy in each class

| **Gender** | **Speed** | **Accuracy** |
|---|---|---|
| Female | High | 99.3% |
| | Medium | 99.3% |

| | | |
|---|---|---|
| Male | Slow | 99% |
| | High | 99.3% |
| | Medium | 99.4% |
| | Slow | 99.4% |
| Average | | 99.28% ±0.018% |

### 3-2-2- Step Length Estimation

The parameters of Weinberg and Ladetto s algorithms were estimated according to pedestrians' walking speeds and their characteristics including gender and height. In Table (7), estimated values of the K factor in the Weinberg algorithm of various walking speeds are reported. According to Table (7), the K coefficient in Weinberg's step length model is different for each gender and walking speed. The K value increased with walking speed. Furthermore, the K value of males was higher than that of those of females at the same speed. In Table (8), estimated values of the P00, P01, and P02 in the Ladetto algorithm of various walking speeds are reported.

Table 7. Estimated K factor in the Weinberg method

| Gender | Speed | Estimated K |
|---|---|---|
| Female | High | 0.42 |
| | Medium | 0.39 |
| | Slow | 0.37 |
| Average | | 0.393 |
| Male | High | 0.45 |
| | Medium | 0.41 |
| | Slow | 0.38 |
| Average | | 0.414 |

Table 8. Estimated coefficients in the Ladetto method

| Gender | Speed | $P_{00}$ | $P_{10}$ | $P_{01}$ |
|---|---|---|---|---|
| Female | High | 1.56 | -0.407 | -0.000195 |
| | Medium | 0.37 | 0.242 | -0.00014 |
| | Slow | 1.08 | -0.312 | -0.00016 |
| Male | High | 1.58 | -0.529 | 0.00832 |
| | Medium | 1.08 | -0.287 | 0.00078 |
| | Slow | 0.91 | -0.226 | -0.0023 |

### 3-3-Positioning Experiments and Evaluation

The experiments took place at the University of Tehran, School of Surveying and Geospatial Engineering in Iran. As can be seen in Figure (5), the experimenter moved along a 25.8 m rectangular path using a Samsung Galaxy S4 at three different speeds. To assess the positioning accuracy, a group of six individuals was chosen for the experiment consisting of three males and three females of varying ages and heights. The average age for men was 31.2 years old and an average height of 179.4 cm, while the average age for women was 27.4 years old and an average height of 165.9 cm. Also, the initial point of the test was known in advance.

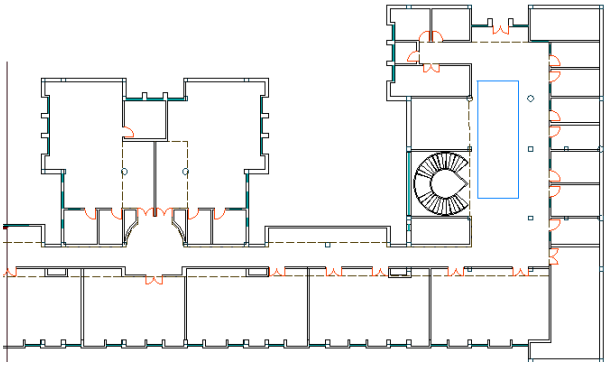

Figure 5. Experiment's 2D plan

In Table (9), the relative error of step length when effective parameters, such as walking speeds and genders, were ignored is compared with the proposed method that considered these factors. According to Table (9), consideration of walking speed and gender improved the accuracy of step length estimation.

Table 9. Comparison of step length estimation error considering and ignoring walking speed and gender

| Step Length Method | Relative Error of Step Length | |
|---|---|---|
| | With Classification (%) | Without Classification (%) |
| Weinberg | 2.48% | 9.52% |
| Ladetto | 1.95% | 9.98% |

Figure (6) shows the relative error of step length estimation of the Weinberg model and Ladetto model for both males and females at slow, medium, and high walking speeds. The mean relative error of the proposed method making use of Weinberg's model and Ladetto algorithms was 2.48% and 1.95%, respectively.

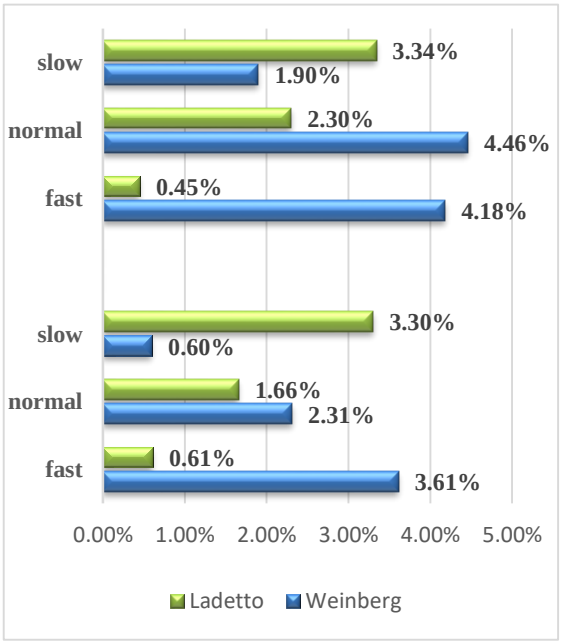


Figure 6. Comparison of relative error of step length estimation of Weinberg and Ladetto methods in different walking speeds and genders.

The mean and STD of the heading estimation error using

the EKF were 2.97 degrees and 2.99 degrees, respectively. According to Figure (7), during fast walking, the body fluctuates the most, leading to the highest heading estimation error of 3.96 degrees.

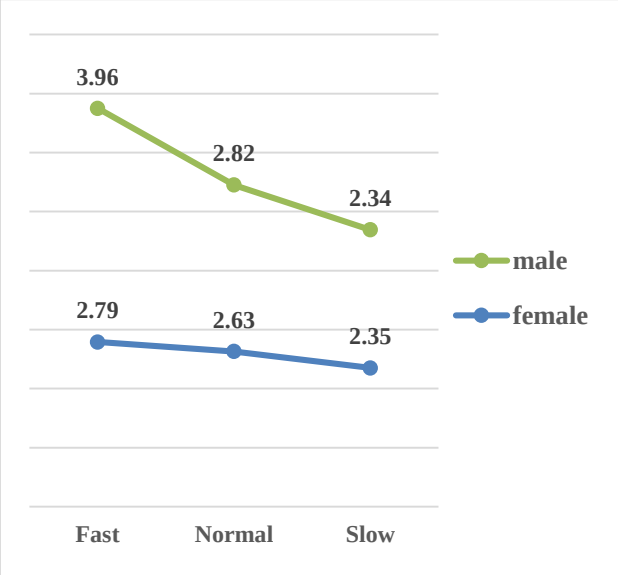


Figure 7. Heading estimation error of EKF method of different walking speeds and genders.

As shown in Figure (8), walking at high speeds results in a higher cumulative error in heading estimation using the EKF algorithm, as compared to walking at medium and low speeds.

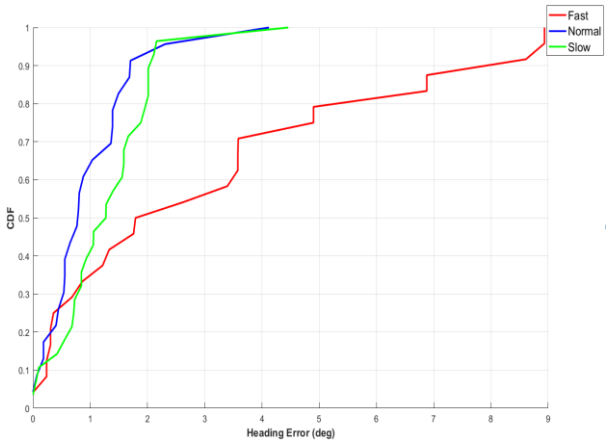


Figure 8. Comparison of the cumulative error of heading estimation with the EKF algorithm at different walking speeds

Figure (9) shows the estimated routes of different experiments with different walking speeds. As shown in Figure (9), in each considered walking speed and gender, three estimated paths were close to the designed path. The calculated errors for step length, heading, and position estimation are shown in Table (10). According to Table (10), along a 25.8-meter path, using the Weinberg method for step length estimation, the average absolute and relative positioning errors were 0.76 and 2.95%, respectively. Moreover, using the Ladetto method for step length estimation, the average absolute and relative positioning errors were 0.92 and 3.57%, respectively.

Table 10. Experiment results on the rectangular path

| **Method** | **Gender** | **Speed** | **Step Length** | **Heading Estimation** | | **Position Estimation** | |
|---|---|---|---|---|---|---|---|
| | | | **Relative Error** | **Mean** | **STD** | **Absolute Error** | **Relative Error** |
| Weinberg | Female | Fast | 3.61% | 3 | 3.1 | 0.93 | 3.59% |
| | | Medium | 2.31% | 3.04 | 4.35 | 0.81 | 3.15% |
| | | Slow | 0.6% | 2.4 | 2.1 | 0.9 | 3.51% |
| | Male | Fast | 4.18% | 5.47 | 3.72 | 0.41 | 1.58% |
| | | Medium | 4.46% | 2.85 | 2.73 | 1.05 | 4.06% |
| | | Slow | 1.9% | 2.25 | 2.03 | 0.46 | 1.8% |
| | Average | | 2.48% | 3.17 | 3 | 0.76 | 2.95% |
| Ladetto | Female | Fast | 0.61% | 3 | 3.1 | 0.63 | 2.44% |
| | | Medium | 1.66% | 3.17 | 4.34 | 1.04 | 4.01% |
| | | Slow | 3.3% | 2.4 | 2.1 | 1.27 | 4.87% |
| | Male | Fast | 0.45% | 5.47 | 3.72 | 1.19 | 4.58% |
| | | Medium | 2.3% | 2.89 | 2.73 | 1.11 | 4.26% |
| | | Slow | 3.34% | 2.25 | 2.03 | 0.33 | 1.29% |
| | Average | | 1.95% | 3.21 | 3 | 0.92 | 3.57% |

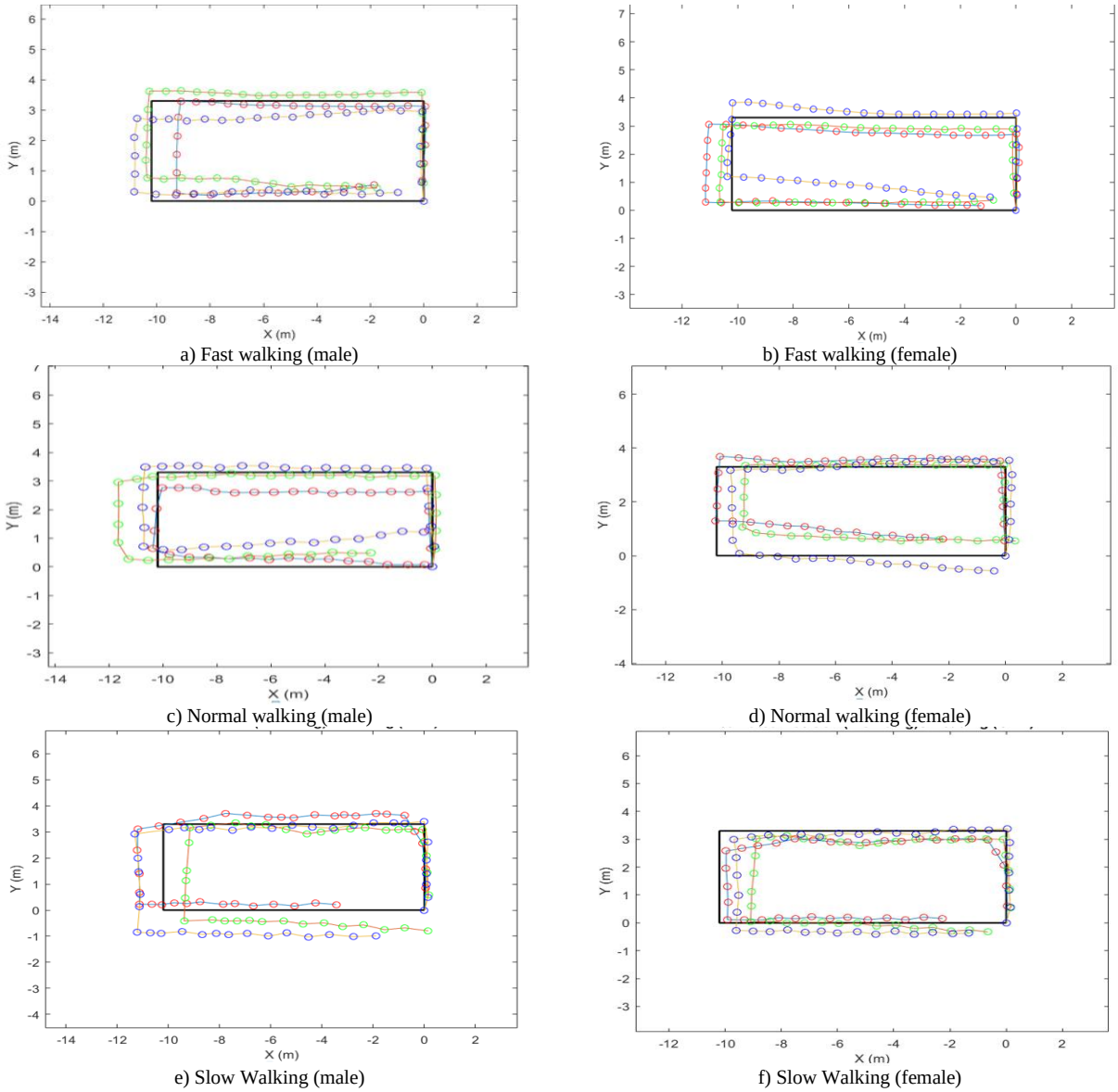


a) Fast walking (male) b) Fast walking (female)

c) Normal walking (male) d) Normal walking (female)

e) Slow Walking (male) f) Slow Walking (female)

Figure 9. Estimated paths of various speeds and genders

## 4- Conclusion

In this paper, the step length model parameters were calculated based on different variables such as pedestrians' walking speeds and genders to increase the accuracy of step length estimation. This strategy consisted of two primary components, data classification, and estimation of PDR parameters. Accordingly, data were divided into six categories based on speed (high, medium, low) and gender (female, male). Additionally, K-Nearest Neighbor was utilized for determining the pedestrian's walking speeds and gender with an overall classification accuracy of 93.2%. In addition, Weinberg and Ladetto algorithms were utilized for step-length estimation. According to the experimental result, the values of the parameters associated with the step length model increased as the walking speed increased, and these parameters were greater for males than for females. The step length estimating errors of the Weinberg method and Ladetto method were 2.48% and 1.95% respectively. In addition, for heading estimation, the EKF was used. The position was calculated by utilizing the estimated heading and step length, and it was determined that the average positioning error was 2/95%. This study demonstrates the significant impact of considering gender and walking speed on step length estimation and indoor positioning accuracy.

## References

Bencak, P., Hercog, D., & Lerher, T. (2022). Indoor Positioning System Based on Bluetooth Low Energy Technology and a Nature-Inspired Optimization Algorithm. *Electronics*, *11*(3), 308.

Daníş, F. S., Cemgíl, A. T., & Ersoy, C. (2021). Adaptive sequential Monte Carlo filter for indoor positioning and tracking with bluetooth low energy beacons. *IEEE Access*, *9*, 37022-37038.

Deng, Z.-A., Hu, Y., Yu, J., & Na, Z. (2015). Extended Kalman filter for real time indoor localization by

fusing WiFi and smartphone inertial sensors. *Micromachines*, *6*(4), 523-543.

Diebel, J. (2006). Representing attitude: Euler angles, unit quaternions, and rotation vectors. *Matrix*, *58*(15-16), 1-35.

Díez, L. E., Bahillo, A., Otegui, J., & Otim, T. (2018). Step length estimation methods based on inertial sensors: A review. *IEEE Sensors Journal*, *18*(17), 6908-6926.

Einicke, G. A., & White, L. B. (1999). Robust extended Kalman filtering. *IEEE Transactions on Signal Processing*, *47*(9), 2596-2599.

Elhoushi, M., Georgy, J., Noureldin, A., & Korenberg, M. J. (2015). Motion mode recognition for indoor pedestrian navigation using portable devices. *IEEE Transactions on Instrumentation and Measurement*, *65*(1), 208-221.

Fang, S.-H., Liao, H.-H., Fei, Y.-X., Chen, K.-H., Huang, J.-W., Lu, Y.-D., & Tsao, Y. (2016). Transportation modes classification using sensors on smartphones. *Sensors*, *16*(8), 1324.

Goyal, P., Ribeiro, V. J., Saran, H., & Kumar, A. (2011). Strap-down pedestrian dead-reckoning system. 2011 international conference on indoor positioning and indoor navigation,

Groves, P. D. (2015). Principles of GNSS, inertial, and multisensor integrated navigation systems, [Book review]. *IEEE Aerospace and Electronic Systems Magazine*, *30*(2), 26-27.

Gu, F., Khoshelham, K., Yu, C., & Shang, J. (2018). Accurate step length estimation for pedestrian dead reckoning localization using stacked autoencoders. *IEEE Transactions on Instrumentation and Measurement*, *68*(8), 2705-2713.

Huang, C., Zhang, F., Xu, Z., & Wei, J. (2022). Adaptive Pedestrian Stride Estimation for Localization: From Multi-Gait Perspective. *Sensors*, *22*(8), 2840.

Huang, L., Li, H., Yu, B., Gan, X., Wang, B., Li, Y., & Zhu, R. (2020). Combination of smartphone MEMS sensors and environmental prior information for pedestrian indoor positioning. *Sensors*, *20*(8), 2263.

Jang, H.-J., Kim, J. W., & Hwang, D.-H. (2007). Robust step detection method for pedestrian navigation systems. *Electronics Letters*, *43*(14), 1.

Jin, Y., Toh, H.-S., Soh, W.-S., & Wong, W.-C. (2011). A robust dead-reckoning pedestrian tracking system with low cost sensors. 2011 IEEE International Conference on Pervasive Computing and Communications (PerCom),

Jurman, D., Jankovec, M., Kamnik, R., & Topič, M. (2007). Calibration and data fusion solution for the miniature attitude and heading reference system. *Sensors and Actuators A: Physical*, *138*(2), 411-420.

Khalili, B., Ali Abbaspour, R., Chehreghan, A., & Vesali, N. (2022). A context-aware smartphone-based 3D indoor positioning using pedestrian dead reckoning. *Sensors*, *22*(24), 9968.

Kim, J. W., Jang, H. J., Hwang, D.-H., & Park, C. (2004). A step, stride and heading determination for the pedestrian navigation system. *Journal of Global Positioning Systems*, *3*(1-2), 273-279.

Klein, I., Solaz, Y., & Ohayon, G. (2018). Pedestrian dead reckoning with smartphone mode recognition. *IEEE Sensors Journal*, *18*(18), 7577-7584.

Ladetto, Q. (2000). On foot navigation: continuous step calibration using both complementary recursive prediction and adaptive Kalman filtering. Proceedings of the 13th International Technical Meeting of the Satellite Division of The Institute of Navigation (ION GPS 2000),

Li, F., Chunshui, Z., Ding, G., Gong, J., Liu, C., & Zhao, F. (2012). A reliable and accurate indoor localization method using phone inertial sensors. Proceedings of the 2012 ACM conference on ubiquitous computing,

Li, W., Chen, R., Yu, Y., Wu, Y., & Zhou, H. (2021). Pedestrian dead reckoning with novel heading estimation under magnetic interference and multiple smartphone postures. *Measurement*, *182*, 109610.

Lu, W., Wu, F., Zhu, H., & Zhang, Y. (2020). A step length estimation model of coefficient self-determined based on peak-valley detection. *Journal of Sensors*, *2020*.

Luo, J., Zhang, C., & Wang, C. (2020). Indoor multi-floor 3D target tracking based on the multi-sensor fusion. *IEEE Access*, *8*, 36836-36846.

Martinelli, A., Gao, H., Groves, P. D., & Morosi, S. (2017). Probabilistic context-aware step length estimation for pedestrian dead reckoning. *IEEE Sensors Journal*, *18*(4), 1600-1611.

Metge, J., Mégret, R., Giremus, A., Berthoumieu, Y., & Décamps, T. (2014). Calibration of an inertial-magnetic measurement unit without external equipment, in the presence of dynamic magnetic disturbances. *Measurement Science and Technology*, *25*(12), 125106.

Moreno-Torres, J. G., Sáez, J. A., & Herrera, F. (2012). Study on the impact of partition-induced dataset shift on $ k $-fold cross-validation. *IEEE Transactions on Neural Networks and Learning Systems*, *23*(8), 1304-1312.

Munoz Diaz, E., de Ponte Müller, F., & García Domínguez, J. J. (2017). Use of the magnetic field for improving gyroscopes' biases estimation. *Sensors*, *17*(4), 832.

Nilsson, J.-O., Zachariah, D., Skog, I., & Händel, P. (2013). Cooperative localization by dual foot-mounted inertial sensors and inter-agent ranging. *EURASIP Journal on Advances in Signal Processing*, *2013*(1), 1-17.

Olivares, A., Ruiz-Garcia, G., Olivares, G., Górriz, J. M., & Ramirez, J. (2013). Automatic determination of validity of input data used in ellipsoid fitting MARG calibration algorithms. *Sensors*, *13*(9), 11797-11817.

Otim, T., Bahillo, A., Díez, L. E., Lopez-Iturri, P., & Falcone, F. (2020). Towards sub-meter level UWB indoor localization using body wearable sensors. *IEEE Access*, *8*, 178886-178899.

Ozyagcilar, T. (2012). Calibrating an ecompass in the presence of hard and soft-iron interference. *Freescale Semiconductor Ltd*, 1-17.

Pratama, A. R., & Hidayat, R. (2013). Performance testing of PDR using common sensors on a smartphone. 2013 International Conference on Advanced Computer Science and Information Systems (ICACSIS),

Pylvänäinen, T. (2008). Automatic and adaptive calibration of 3D field sensors. *Applied Mathematical Modelling*, *32*(4), 575-587.

Sheu, J. S., Huang, G. S., Jheng, W. C., & Hsiao, C. H. (2014). Design and implementation of a three-dimensional pedometer accumulating walking or jogging motions. 2014 International Symposium on Computer, Consumer and Control,

Weinberg, H. (2002). Using the ADXL202 in pedometer and personal navigation applications. *Analog Devices AN-602 application note*, *2*(2), 1-6.

Woodman, O. J. (2007). *An introduction to inertial navigation*.

Wu, B., Ma, C., Poslad, S., & Selviah, D. R. (2021). An adaptive human activity-aided hand-held smartphone-based pedestrian dead reckoning positioning system. *Remote Sensing*, *13*(11), 2137.

Wu, D., Xia, L., & Geng, J. (2018). Heading estimation for pedestrian dead reckoning based on robust adaptive Kalman filtering. *Sensors*, *18*(6), 1970.

Yang, C., & Shao, H.-R. (2015). WiFi-based indoor positioning. *IEEE Communications Magazine*, *53*(3), 150-157.

Zhao, H., Zhang, L., Qiu, S., Wang, Z., Yang, N., & Xu, J. (2019). Pedestrian dead reckoning using pocket-worn smartphone. *IEEE Access*, *7*, 91063-91073.

Zhou, N., Lau, L., Bai, R., & Moore, T. (2021). Novel prior position determination approaches in particle filter for ultra wideband (UWB)-based indoor positioning. *NAVIGATION: Journal of the Institute of Navigation*, *68*(2), 277-292.

Zhuang, Y., Lan, H., Li, Y., & El-Sheimy, N. (2015). PDR/INS/WiFi integration based on handheld devices for indoor pedestrian navigation. *Micromachines*, *6*(6), 793-812.